

PATTERN DISCOVERY IN TIME-COURSE OMICS DATA USING NON-NEGATIVE CP TENSOR DECOMPOSITION (NCPD)

Shoaib Bin Masud ¹ Anna Konstorum ² Misha Kilmer ³ Shuchin Aeron ¹

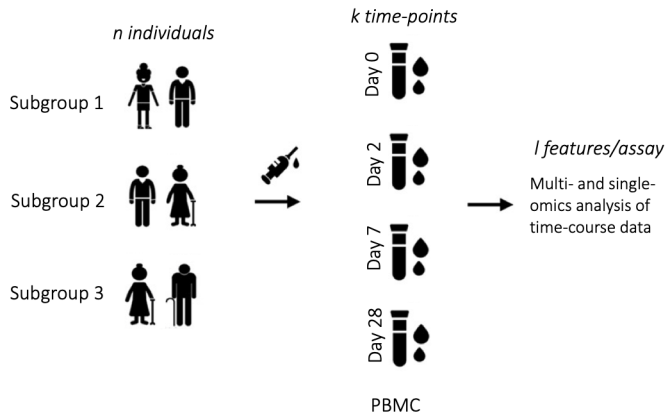
¹Department of ECE, Tufts University

²Department of Pathology, Yale School of Medicine

³Department of Mathematics, Tufts University

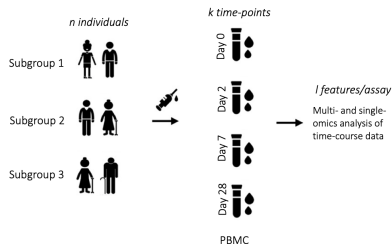
February 26, 2023

VACCINATION RESPONSE DATA STRUCTURE



- Subgroups of individuals of interest to researchers (e.g. age, sex, living-condition) are vaccinated at day 0, and samples are collected pre-vaccination (day 0), and at time-points post-vaccination.
- Total of $I \times n \times k$ data points

VACCINATION RESPONSE DATA STRUCTURE



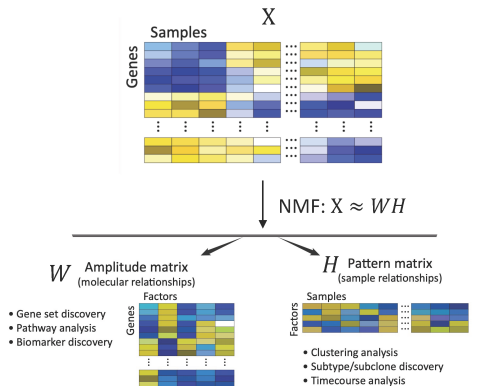
- Total of $n \times k \times I$ data points
- Want to answer questions including:
 - Are there different subgroups of individuals that respond differently to the vaccine (either the pre-determined subgroups, or other clusters)?
 - Which genes are most active in the response?
 - Are there additional covariates that mitigate response signature? (e.g. demographics, experiment,...)

NON-NEGATIVE MATRIX FACTORIZATION (NMF)

Recall that for a non-negative matrix, $\mathbf{X}_{n \times m}$, non-negative matrix factorization (NMF) finds a rank R decomposition,

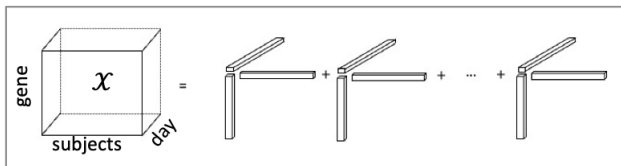
$$\mathbf{X}_{n \times m} \approx \mathbf{W}_{n \times R} \mathbf{H}_{R \times m}$$

- If X is a gene by sample matrix for a given time-point, then each column of W represents a particular co-expressed pattern of gene activation, and each column of H represents the strength of presence of that pattern in a given subject.



(Stein-O'Brien et al., 2018)

NON-NEGATIVE CP DECOMPOSITION (NCPD)



- Non-negative CP decomposition (NCPD) extends the concept of representing a dataset as the sum of rank-one components to ≥ 2 dimensions.
- For a tensor \mathcal{X} of gene expression \times subject \times time data, we can represent \mathcal{X} as

$$\mathcal{X} \approx [[\lambda; A^{(1)}, A^{(2)}, A^{(3)}]] \equiv \sum_{r=1}^R \lambda_r \mathbf{a}_r^{(1)} \circ \mathbf{a}_r^{(2)} \circ \mathbf{a}_r^{(3)}, \quad (1)$$

where $\mathbf{a}_r^{(i)} \geq 0$ and $\|\mathbf{a}_r^{(i)}\|_2 = 1$ for $i = \{1, 2, 3\}$, and λ is the normalization constant.

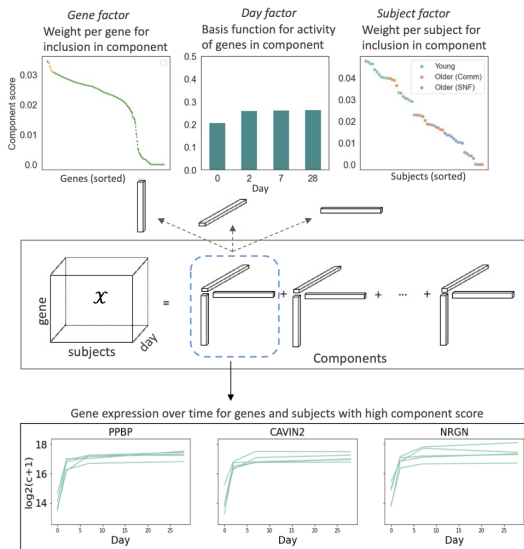
- Denoting $\hat{\mathcal{X}} = [[\lambda; A^{(1)}, A^{(2)}, A^{(3)}]]$, the objective to minimize for tensor decomposition:

$$\min_{\lambda, A^{(1)}, A^{(2)}, A^{(3)} \geq 0} \phi(\mathcal{X}, \hat{\mathcal{X}}), \quad (2)$$

- $\phi(\mathcal{X}, \hat{\mathcal{X}})$ is the loss function e.g., squared Frobenius norm¹ $\phi(\mathcal{X}, \hat{\mathcal{X}}) = \frac{1}{2} \|\mathcal{X} - \hat{\mathcal{X}}\|_F^2$. We denote this decomposition as NCPD-F.

¹Used in CP-OPT/CP-ALS library in Tensor Toolbox

NON-NEGATIVE CP DECOMPOSITION (NCPD): INTERPRETATION



- Performed using CP-OPT library in Tensor Toolbox.

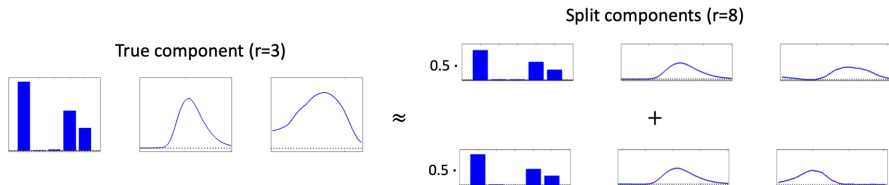
How to choose the number of rank R for decomposition?

- If R is less than the true rank, we risk not being able to detect all patterns in the dataset.
- By setting the number of ranks too high, component splitting may occur. In this case, decomposition will split one pattern into two or more- rendering the analysis of each of these not only uninformative but also misleading.

NON-NEGATIVE CP DECOMPOSITION (NCPD): CHOOSING RANK

COMPONENT SPLITTING IN NCPD-F

- A well-known amino acids data set from Andersson and Bro ².
- Contains fluorescence measurements of 5 samples containing 3 amino acids: Tryptophan, Tyrosine, and Phenylalanine.
- Each amino acid corresponds to a rank-one component.
- The tensor is of size $5 \times 51 \times 201$ from 5 samples, 51 excitations, and 201 emissions.
- When the decomposition rank is set to be *higher* than the true rank, component splitting can occur. Here, a 'true' component from a rank three decomposition is split on the third mode.



²Rasmus Bro, PARAFAC: Tutorial and applications, Chemometrics and Intelligent Laboratory Systems, 1997, 38, 149-171

- We choose the rank R of the model based on the following considerations:

- **Relative Frobenius error**

$$\frac{\|\mathcal{X} - \hat{\mathcal{X}}\|_F^2}{\|\mathcal{X}\|_F^2}$$

- **Similarity score:** For two mode-3 models of same rank R , $\hat{\mathcal{X}}_1 = [[\lambda^1; A^{(1)}, A^{(2)}, A^{(3)}]]$ and $\hat{\mathcal{X}}_2 = [[\lambda^2; B^{(1)}, B^{(2)}, B^{(3)}]]$, similarity score is defined as:

$$S(\hat{\mathcal{X}}_1, \hat{\mathcal{X}}_2) = \max_{\omega \in \Omega} \frac{1}{R} \sum_{i=1}^R \left(1 - \frac{|\lambda_r^1 - \lambda_{\omega(r)}^2|}{\max(\lambda_r^1, \lambda_{\omega(r)}^2)} \right) \prod_{i=1}^3 a_r^{(i)\top} b_{\omega(r)}^{(i)}. \quad (3)$$

- Ω denotes the set of all permutations of the factors, and ω is a particular permutation.
- Similarity score measures robustness of a decomposition across varying initial conditions.
- **max internal n-similarity (mINS):** A new metric to determine whether component splitting has occurred.³

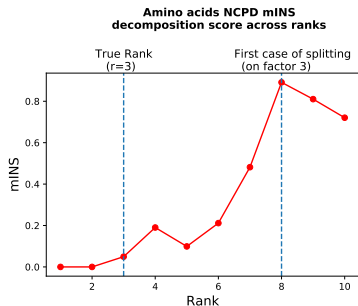
³Developed by Konstorum et. al [1] Kleinstein Lab, Yale University. Manuscript preparation in progress.

NON-NEGATIVE CP DECOMPOSITION (NCPD): CHOOSING RANK

- The *maximum internal n-Similarity* (mINS) is used to assess whether component splitting has occurred in an NCPD.
- For a mode-3 model of rank R , $\hat{\mathcal{X}} = [[\lambda; A^{(1)}, A^{(2)}, A^{(3)}]]$, the mINS is defined as

$$mINS = \max_{i,j,i \neq j} \left(g_{i,j} \left(A^{(1)} \right) \cdot g_{i,j} \left(A^{(2)} \right) \right), \quad (4)$$

where $g_{i,j}(A) = S(a_i, a_j)$ is a similarity measure (such cosine or correlation) between columns i and j in matrix A .



- The plot is generated using CP-OPT library in Tensor Toolbox where *the objective used for the decomposition is the Frobenius norm (NCPD-F)*.

MOTIVATION BEHIND OPTIMAL TRANSPORT-BASED TENSOR FACTORIZATION

- We are thus motivated to modify NCPD so that splitting does not occur before all patterns are identified.
- This is where using the recently proposed optimal transport based tensor factorization namely Wasserstein tensor factorization ⁴ [2] may prove useful.
- Loss function based optimal transport theory incorporates the underlying geometry of the data, thus is able to recover all components without distortions.

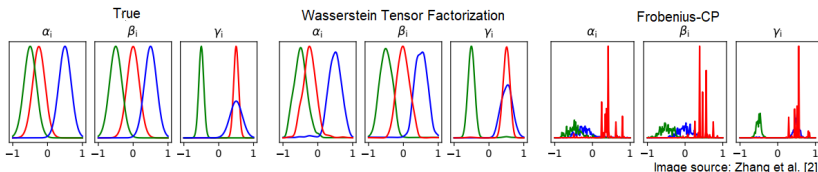


FIGURE: $\mathcal{X}_{\text{True}} = \sum_{i=1}^3 \alpha_i \circ \beta_i \circ \gamma_i$, where $\{\alpha_i, \beta_i, \gamma_i\}_{i=1}^3$ are univariate Gaussian. \circ denotes the outer product of vectors.

⁴Zhang et. al A unified framework for non-negative matrix and tensor factorisations with a smoothed wasserstein loss, <https://arxiv.org/abs/2104.01708>

WASSERSTEIN TENSOR FACTORIZATION

OPTIMAL TRANSPORT

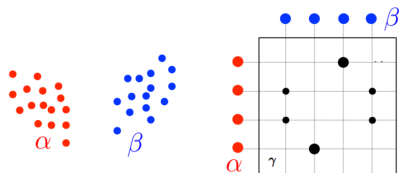


image source: Computational OT by Cuturi and Peyre [2]

- Given α and β are probability distribution supported on a finite set Ω , with $\text{Cardinality}(\Omega) = n$.
- Let $C \in \mathbb{R}^{n \times n}$ be the ground cost matrix with C_{ij} denoting the cost of transporting mass from point i to j . The optimal transport distance is defined via

$$\text{OT}(\alpha, \beta) \stackrel{\text{def}}{=} \min_{\gamma \in \Gamma(\alpha, \beta)} \langle C, \gamma \rangle \stackrel{\text{def}}{=} \min_{\gamma \in \Gamma(\alpha, \beta)} \sum_{i,j}^{n,n} C_{ij} \gamma_{ij} \quad (5)$$

where $\Gamma(\alpha, \beta) = \{\gamma \in \mathbb{R}_{\geq 0}^{n \times n} : \gamma \mathbf{1} = \alpha, \gamma^\top \mathbf{1} = \beta\}$ is the set of all couplings of (α, β) , and γ is the optimal coupling.

- For ground cost C_{ij} , one may choose squared of Euclidean distance between the points in support of α and β (this is also known Wasserstein-2 distance).
- **Drawbacks:** Computationally expensive $\mathcal{O}(n^3)$.

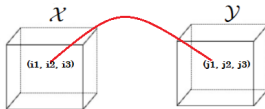
- Entropy regularized optimal transport [3]

$$\text{OT}_\varepsilon(\alpha, \beta) := \inf_{\gamma \in \Gamma(\alpha, \beta)} \langle C, \gamma \rangle + \varepsilon E(\gamma), \quad (6)$$

- $E(\gamma) = \langle \gamma, \log \gamma - 1 \rangle$ is the entropy of the coupling matrix.
- $\varepsilon > 0$ is the entropy regularizer.
- As $\varepsilon \rightarrow 0$, $\text{OT}_\varepsilon \rightarrow \text{OT}$.
- Advantages
 - Smooth and strongly convex.
 - Computationally cheaper, e.g. Sinkhorn algorithm has complexity $\mathcal{O}(n^2 \log n \varepsilon^{-2})$ [4].

WASSERSTEIN TENSOR FACTORIZATION

OT DISTANCE BETWEEN TENSORS



- Given two tensors $\mathcal{X}, \mathcal{Y} \in \mathbb{R}^{n_1 \times n_2 \times n_3}$. Consider $\mathcal{X}, \mathcal{Y} \in \mathcal{P}(\Omega)$, where $\mathcal{P}(\Omega)$ is the set of all probability distributions over the multi-index support set Ω . Optimal transport distance between \mathcal{X} and \mathcal{Y} is,

$$\text{OT}(\mathcal{X}, \mathcal{Y}) := \inf_{\gamma \in \Gamma(\mathcal{X}, \mathcal{Y})} \langle C, \gamma \rangle. \quad (7)$$

- $\Gamma(\mathcal{X}, \mathcal{Y})$ is the set of all possible couplings between \mathcal{X} and \mathcal{Y} and C is the ground cost tensor where $C_{(i_1 i_2 i_3), (j_1 j_2 j_3)}$ denotes the cost to couple point (i_1, i_2, i_3) to (j_1, j_2, j_3) .

$$C_{(i_1 i_2 i_3), (j_1 j_2 j_3)} = \sum_{k=1}^3 C_{i_k, j_k}^{(k)}, \quad (8)$$

where $C^{(k)}$ is the cost matrix for the k th mode of tensor \mathcal{X} .

- Entropic OT between \mathcal{X} and \mathcal{Y}

$$\text{OT}_\varepsilon(\mathcal{X}, \mathcal{Y}) := \inf_{\gamma \in \Gamma(\mathcal{X}, \mathcal{Y})} \langle C, \gamma \rangle + \varepsilon E(\gamma). \quad (9)$$

- Decomposition of tensor $\mathcal{X}_{\geq 0} \in \mathbb{R}^{n_1 \times n_2 \times n_3}$ using entropy regularized optimal transport [2]

$$\min_{\lambda, A^{(1)}, A^{(2)}, A^{(3)} \geq 0} \text{OT}_\varepsilon(\mathcal{X}, [[\lambda; A^{(1)}, A^{(2)}, A^{(3)}]]), \quad (10)$$

where $A^{(i)} \in \mathbb{R}_{\geq 0}^{n_i \times R}$, $i = 1, 2, 3$, $[[\lambda; A^{(1)}, A^{(2)}, A^{(3)}]] \equiv \sum_{r=1}^R \lambda_r \mathbf{a}_r^{(1)} \circ \mathbf{a}_r^{(2)} \circ \mathbf{a}_r^{(3)}$.

- [2] solves the following to decompose \mathcal{X}

$$\min_{\lambda, A^{(1)}, A^{(2)}, A^{(3)}} \text{OT}_\varepsilon(\mathcal{X}, [[\lambda; A^{(1)}, A^{(2)}, A^{(3)}]]) + \sum_{i=1}^3 \rho_i E_{\Sigma_i}(A^{(i)}) \quad (11)$$

where $E_{\Sigma_i}(A^{(i)}) = E(A^{(i)}) + \ell(A^{(i)} \in \Sigma_i)$, Σ_i is the constraint set of $A^{(i)}$ and $\ell(\cdot)$

$$\ell(x \in A) = \begin{cases} 0, & \text{if } x \in A \\ +\infty & \text{otherwise.} \end{cases}$$

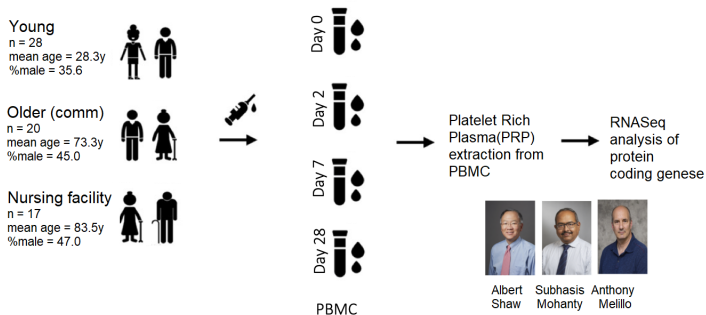
is the indicator function.

- $E(\cdot)$ relaxes the non-negativity constraint.
- Equation 9 is solved by performing *block coordinate descent algorithm in each of the factor matrices individually* [2].
- We denote this decomposition as NCPD-W.

Zhang et al. A unified framework for non-negative matrix and tensor factorisations with a smoothed wasserstein loss,
<https://arxiv.org/abs/2104.01708>

PLATELET RNASeq VACCINATION TIME-COURSE

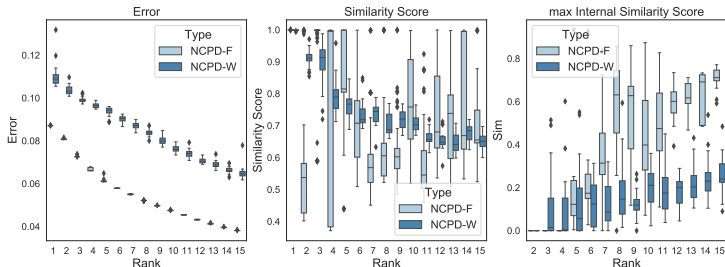
Recruitment: subjects getting the flu vaccine (2018) from three cohorts



- A tensor framework of genes \times subject \times day is used to store the data.
- The final dimensions of the tensor is $500 \times 54 \times 4$. (500 most variable genes, 54 subjects with data for all days.)
- Hyperparameters used in NCPD-W.

Hyperparameter	Value
ϵ	0.1
ρ	0.01
learning rate	1

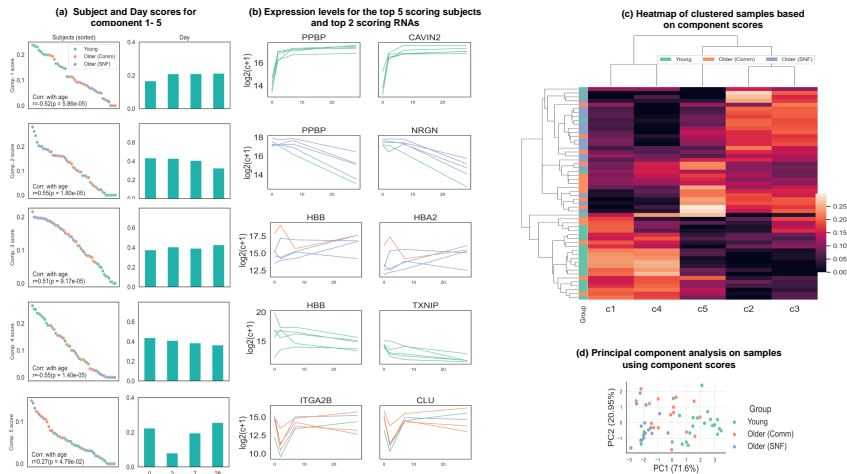
- Comparison between NCPD-F and NCPD-W in terms of normalized Frobenius error, similarity score and mINS.



Observations:

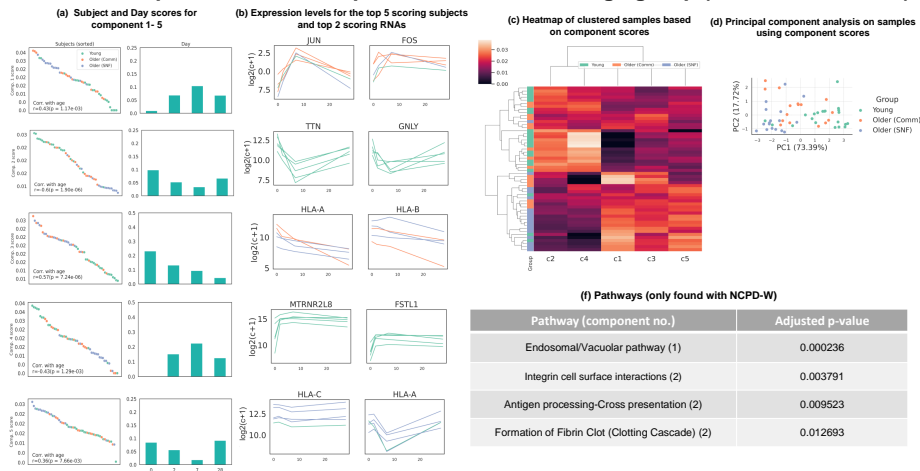
- Error decreases as rank increases for both NCPD-F and NCPD-W. However, for any given rank R , NCPD-W has slightly higher error compared to NCPD-F.
- Similarity score decreases almost monotonically as rank R increases for NCPD-W.
- As rank (R) increases, mINS scores increase for both NCPD-F and NCPD-W.
- mINS scores for NCPD-F are higher than NCPD-W when $R > 5$, which may indicate component splitting for NCPD-F.

Tensor components related to platelet activation and age group (NCPD-F, Rank = 5)



- For $R = 5$, NCPD-F successfully discovers all 5 components with no splitting.
- Subject component scores show a strong association with the three groups (Figure (c) and (d)).

Tensor components related to platelet activation and age group (NCPD-W, Rank = 5)

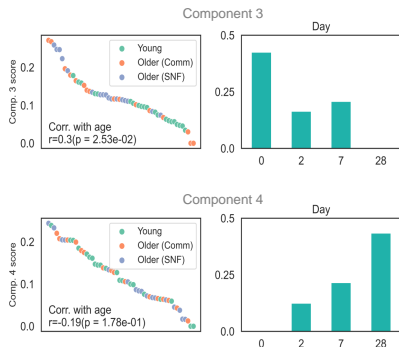


- For $R = 5$, NCPD-W discovers few new patterns ones e.g., 1,2, 4.
- Day scores closely follows the original expression levels for top scoring genes.
- Subject component scores show a strong association with the three groups (Figure (c) and (d)).
- NCPD-W components found association with few new pathways which were not discovered with NCPD-F.

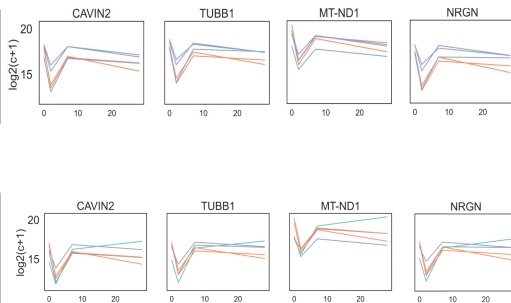
- Effect of component splitting when NCPD-F decomposition with higher rank.

Tensor components related to platelet activation and age group (NCPD-F, Rank = 9)

(a) Subject and day scores for component 3 and 4



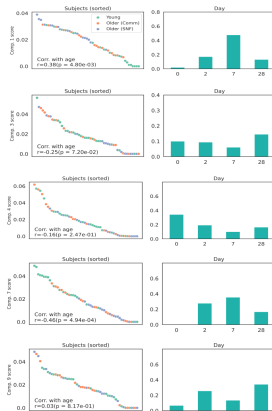
(b) Expression levels for top 5 scoring subjects and top few scoring RNAs



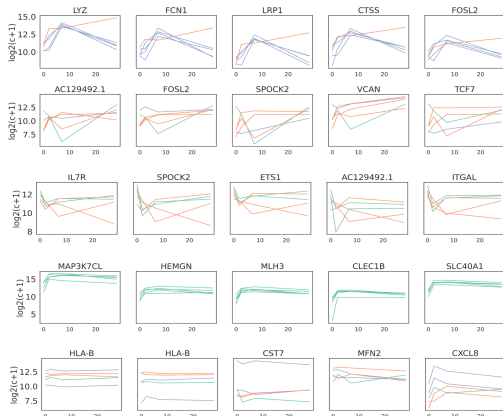
- Day patterns associated with component 3 and 4 do not follow the original gene expression individually.
- Added components will follow the gene expression, which clearly indicates the NCPD-F suffers from component splitting.

Tensor components related to platelet activation and age group (NCPD-W, Rank = 9)

(a) Subject and day scores for component 1,3,4,5,9



(b) Expression levels for the top 5 scoring subjects and few scoring RNAs



- Day pattern follow the trend of the expression of most of the top scoring genes.
- NCPD-W is able to avoid component splitting which may help to discover new patterns.

- Propose using optimal transport based tensor decomposition (NCPD-W) for the omics-time course data.
- Shown that NCPD-W can discover patterns which are not discovered by NCPD-F for the rank 5 decomposition.
- Shown that For higher rank decomposition, NCPD-W shows less component splitting compared to NCPD-F.

- Finding the appropriate set of hyperparameters for NCPD-W in order to improve the decomposition quality.
- Understanding why some genes (like the HLAs in this study), do not follow patterns.
- For NCPD-W, search for another ground cost function which can act as prior in order to reduce component splitting.
- Adding regularization in the tensor decomposition objective function in order to reduce component splitting.

*Yale University
Yale School of Medicine*



*Department of Pathology
Steven Kleinstein
Anna Konstorum*

Tufts University



*Dept. of Mathematics
Misha Kilmer*

*Dept. Electrical & Computer Engineering
Shuchin Aeron*

Thank you!

Questions?

Shoaib Bin Masud

supported by
U.S. Army DEVCOM Soldier Center
Cooperative Agreement Number
W911QY-19-2-0003.

- [1] A Konstorum, S Mohanty, Y Zhao, A Melillo, B Vander Wyk, A Nelson, S Tsang, TP Blevins, RB Belshe, DG Chawla, et al.
Platelet response to influenza vaccination reflects effects of aging.
bioRxiv, 2022.
- [2] Stephen Y Zhang.
A unified framework for non-negative matrix and tensor factorisations with a smoothed wasserstein loss.
In *Proceedings of the IEEE/CVF International Conference on Computer Vision*, pages 4195–4203, 2021.
- [3] Marco Cuturi.
Sinkhorn distances: Lightspeed computation of optimal transport.
Advances in neural information processing systems, 26, 2013.
- [4] Gabriel Peyré, Marco Cuturi, et al.
Computational optimal transport: With applications to data science.
Foundations and Trends® in Machine Learning, 11(5-6):355–607, 2019.